Particuology xxx (2012) xxx–xxx

Contents lists available at SciVerse ScienceDirect

Particuology

journal homepage: www.elsevier.com/locate/partic

Evolution of planetary boundary layer under different weather conditions, and its impact on aerosol concentrations

Jiannong Quan[a,b], Yang Gao[a], Qiang Zhang[a], Xuexi Tie[c,d,*], Junji Cao[c], Suqin Han[e], Junwang Meng[a], Pengfei Chen[a], Delong Zhao[a]

[a] Beijing Weather Modification Office, Beijing, China
[b] Institude of Urban Meteorology, CMA, Beijing, China
[c] Key Laboratory of Aerosol, SKLLQG, Institute of Earth Environment, Chinese Academy of Sciences, Xian, China
[d] National Center for Atmospheric Research, Boulder, USA
[e] Tianjin Institute of Meteorological Sciences, Tianjin, China

ARTICLE INFO

Article history:
Received 9 January 2012
Received in revised form 2 April 2012
Accepted 26 April 2012

Keywords:
Planetary boundary layer (PBL)
Interaction between the PBL and aerosols

ABSTRACT

A field experiment was conducted in Tianjin, China from September 9–30, 2010, focused on the evolution of Planetary Boundary Layer (PBL) and its impact on surface air pollutants. The experiment used three remote sensing instruments, wind profile radar (WPR), microwave radiometer (MWR) and micro-pulse lidar (MPL), to detect the vertical profiles of winds, temperature, and aerosol backscattering coefficient and to measure the vertical profiles of surface pollutants (aerosol, CO, SO_2, NO_x), and also collected sonic anemometers data from a 255-m meteorological tower. Based on these measurements, the evolution of the PBL was estimated. The averaged PBL height was about 1000–1300 m during noon/afternoon-time, and 200–300 m during night-time. The PBL height and the aerosol concentrations were anti-correlated during clear and haze conditions. The averaged maximum PBL heights were 1.08 and 1.70 km while the averaged aerosol concentrations were 52 and 17 $\mu g/m^3$ under haze and clear sky conditions, respectively. The influence of aerosols and clouds on solar radiation was observed based on sonic anemometers data collected from the 255-m meteorological tower. The heat flux was found significantly decreased by haze (heavy pollution) or cloud, which tended to depress the development of PBL, while the repressed structure of PBL further weakened the diffusion of pollutants, leading to heavy pollution. This possible positive feedback cycle (more aerosols → lower PBL height → more aerosols) would induce an acceleration process for heavy ground pollution in megacities.

1. Introduction

The planetary boundary layer (PBL) is the lowest part of the troposphere and plays important roles in affecting atmospheric environment and human's life. Because air pollution concentrations are generally emitted from surface, and strongly constrained in the PBL, the air pollutants are significantly higher in the PBL than the rest of the atmosphere (Hayden et al., 1997; Hoff et al., 1996; Strawbridge & Snyder, 2004; Zhang, Ma, Tie, Huang, & Zhao, 2009; Zhang, Quan, Tie, Huang, & Ma, 2011). The evolution of the PBL height plays important roles for the long-range transport, and regulates the diurnal variability of air pollutants in large cities (Tie et al., 2007; Ying, Tie, & Li, 2009). Thus, better understanding of the evolution of PBL is an essential issue for the interpretation of atmospheric constituents (Bright & Mullen, 2002). In addition, the evolution of the PBL is also an important factor for making weather forecasting, and it is a key parameter for determining the extent of turbulence and dispersion for pollutants (Dabberdt et al., 2004).

Measurements of PBL are difficult tasks due to its complicated vertical structure. Recently, some remote sensing instruments, for example, boundary wind profile radar (BWPR) (Wyngaard, 1990), microwave radiometers (MR) (Guldner & Spankuch, 1999), and micro-pulse lidar (MPL) become available and were used to measure the vertical structure of wind, temperature, and aerosols in the PBL (Clifford, Kaimal, Lataitis, & Strauch, 1994; Westwater et al., 1999; Wilczak, Gossard, Neff, & Eberhard, 1996). These instruments can detect the vertical structures of dynamic and thermodynamic of PBL, and pollutants in the PBL, which are suitable for studying the evolution of the PBL. Due to the fact that the detection of the PBL by different instruments uses different methods, depending on which physical processes are used, thus, the comparison of the results of

* Corresponding author at: Key Laboratory of Aerosol, SKLLQG, Institute of Earth Environment, Chinese Academy of Sciences, Xian, China.
E-mail address: xxtie@ucar.edu (X. Tie).

1674-2001/$ – see front matter © 2012 Chinese Society of Particuology and Institute of Process Engineering, Chinese Academy of Sciences. Published by Elsevier B.V. All rights reserved.
http://dx.doi.org/10.1016/j.partic.2012.04.005

these instruments is needed to better understand the structure of PBL and their evolution.

In this study, we have carried out comprehensive measurements of the PBL in Tianjin, China during the period from 9 to 30 September 2010. In addition, a series of measurements of aerosol particles and pollution gases (CO, SO_2, and NO_x) as well as the heat and momentum fluxes on a 255 m meteorological tower was also conducted to study the interaction between the PBL and air pollutants. The analysis of this field experiment will focus on the following important issues, including (a) to define the PBL height in Tianjin by comparing the difference of PBL heights measured by different instruments (i.e., boundary wind profile radar, microwave radiometers, and micro-pulse lidar), (b) to study the PBL under different meteorological conditions (such as haze and cloud), and (c) to study the effect of the PBL on air pollutants.

2. Experiment and instruments

A comprehensive field experiment was carried out between 9 and 30 September 2010, in Tianjin, China. The focus of the experiment is to study the vertical structure of the PBL and the interaction between the PBL and the surface air pollutants (such as aerosol, SO_2, CO, and NO_x). Tianjin is a municipality directly under the Central Government, and it is situated in the eastern part of the North China Plain (NCP), covering an area of 11,300 km^2 and with a population of 8 million. Tianjin is a heavily industrial city, including petroleum, natural gas, and sea salt along the coastal area. Due to the rapid economical development in recent years, the air pollution has become a serious problem in the city. The measurement site is located in the atmospheric boundary layer observation station in Tianjin (39°04′N, 117°12′E), which is a residential and traffic mixing area between the Second Ring Road and Outer Ring Road. There is a residential district on the southwest side, a busy road from the east, and an expressway about 150 m from the north.

During the experiment period, three remote sensing instruments, i.e., boundary wind profile radar (Airda-3000, Airda Co., China), microwave radiometers (MP-3000A, Radiometrics Co., USA), and micro-pulse lidar (MPL-4B, Sigmaspace Co., USA), were employed to study the evolution of PBL. The detailed information regarding these three instruments is described as follows. (a) The PRF (pulse repetition frequency) of the MPL is 2500 Hz, with a wavelength of 532 nm of the laser beam. The peak value of the optical energy of laser beam is 8 μJ. The pulse duration ranges from 10 to 100 ns, and the pulse interval was set to 200, 500, 1000 and 2000 ns, corresponding to a spatial resolution of 30, 75, 150 and 300 m, respectively. (b) The Airda-3000 is a boundary wind profile radar which uses refractive index fluctuations of the air, producing mainly by turbulence. The working frequency is 1290 MHz, and detecting accuracy is ≤1 m/s for horizontal wind, ≤0.3 m/s for vertical wind, and ≤10° for wind direction. The radar can measure vertical distribution of wind with altitude range between 50 and 3450 m. The vertical resolution is 50 m for altitude lower than 500 m, and 100 m for altitude higher than 500 m. (c) The Radiometrics MP-3000A Microwave Profiler is a rugged hyper-spectral microwave radiometer that measures vertical profiles of temperature, humidity, and liquid water. These profiles extend from the surface up to 10 km in altitude. The instrument used 21 K-band (22–30 GHz) and 14 V-band (51–59 GHz) microwave frequency channels, as well as one 10 μm infrared channel. The vertical resolution is 50 m for 0–0.5 km, 100 m for 0.5–2 km, and 250 m for 2–10 km.

In addition to the vertical profile measurements, several surface air pollutant instruments were used, for measuring aerosol (with different size bins), CO, SO_2, NO, NO_2, and NO_x concentrations. The aerosol number concentrations with bin size from 10 to 662 nm were measured by a scanning mobility particle sizer (SMPS, Model 3936, TSI, USA) with a time resolution of 5 min. The SMPS consists of a differential mobility analyzer (DMA, Model 3081) and a condensation particle counter (CPC, Model 3772). The sheath and sample flows of the DMA were 3 L/min and 0.3 L/min, respectively. The ambient aerosol sample passes through a silica gel diffusion drier, with relative humidity (RH) maintained below 40%. The aerosol sample then passes into an air-conditioned measurement container, with a temperature maintained around 20 °C. NO–NO_2–NO_x was measured with a chemiluminescent trace level analyzer (TEI; Model 42iTL). The analyzer has a detection limit of 0.025 ppbv. CO was measured by the Model 48iTL enhanced CO analyzer, using a gas filter correlation technology, with a detection limit of 0.04 ppmv. Sulfur dioxide (SO_2) was detected with a pulsed UV fluorescence analyzer (TEI; Model 43 i-TLE). The detection limit for this analyzer is 0.05 ppbv for 2-min integration with a precision of about 0.20 ppbv. Finally, the turbulence fluxes were also measured during the experiment, with a sonic anemometer (CSAT-3D), which was mounted on a 220 m of the meteorological tower in the site. The detection frequency is 50 Hz. These high frequencies of temperature (T), winds (U, V, and W) can be used to calculate the heat flux (Q), and momentum flux (such as turbulence kinetic energy (TKE)), which are important factors for determing the evolution of the PBL (Liu, Peters, & Foken, 2001; Schotanus, Nieuwstadt, & de Bruin, 1983)

3. Results and analysis

3.1. Measured characterization of the PBL

The height of the PBL can be defined in several ways, dependent upon the measurement method of instruments. For example, it can be determined by temperature inversion layer, changes in air mass, humidity profiles, and rapid changes in wind speed and/or a change in wind direction. These characters are all related to each others. For example, an inversion layer can trap air mass within the PBL, which limits the exchange of air mass and air energy between the PBL and the free troposphere. In some cases, for example, during a week PBL case, the transition between the PBL and free atmosphere is not easy to be defined. In this study, we have an advantage to use three instruments to define the PBL, which shows some useful information regarding the determination of the PBL by different parameters. The detailed information for determining the PBL height by the 3 instruments are described as follows. (1) For the MWR instrument, the top of the PBL is estimated at the altitude where there is a rapid and large change in the dew point (Geng et al., 2009; Wilczak et al., 1996). The dew point is determined by air temperature and relative humidity. When there is a large change in the dew point, where temperature is at coldest and humidity is rapidly reduced, the top of the PBL is defined (Wilczak et al., 1996). (2) For the WPR instrument, the PBL height is estimated at the altitude where there is a strong variation in horizontal wind (Wyngaard, 1990). During daytime, the PBL height is defined as the position where a strong wind shear occurs. During nighttime, the nocturnal PBL over land is usually stably stratified as a result of surface radiative cooling. (3) For the MPL instrument, the PBL height is determined at the altitude where a sudden decrease in the scattering coefficient occurs (Boers & Eloranta, 1986; Brooks, 2003; Cohn & Angevine, 2000). The fundamental premise takes advantage of the large gradient in aerosol concentration that is generally evident between the boundary layer aerosols and those found in the free troposphere. The entrainment zone is the transition zone between the PBL and the free troposphere and depending on the time of day

Please cite this article in press as: Quan, J., et al. Evolution of planetary boundary layer under different weather conditions, and its impact on aerosol concentrations. *Particuology* (2012), http://dx.doi.org/10.1016/j.partic.2012.04.005

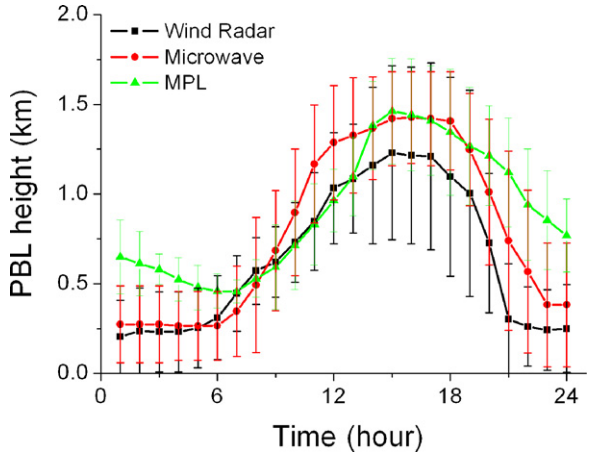

Fig. 1. Averaged diurnal variation of the PBL measured by WPR, MWR, and MPL in Tianjin, China from 9 to 30 September.

can be highly variable. The top of the PBL, in the idealized case, is therefore taken to be the midway point of the entrainment zone.

Fig. 1 shows the averaged diurnal variation of the PBL height measured by the WPR, MWR, and MPL instruments in Tianjin, China during the period from 9 to 30 September 2009. During strong wind and rain events of the experiment, when the height of PBL cannot be clearly defined, the calculation of the PBL height is excluded. The result suggests that during the morning period, the PBL heights measured by WPR and MWR are consistent, with an averaged PBL height of 250 m between middle-night to 6 AM. After 6 AM, the PBL starts to rapidly increase. At noontime, the PBL height reaches to about 1000–1200 m. After 6 PM, the PBL height starts to rapidly decrease. At 9 PM, the PBL height decreases to about 250 m measured by WPR. The PBL height measured by MWR is somewhat slowly decreased as compared to the WPR result. For example, measured PBL height reaches a minimum value (300 m) at 11 PM, which is about 2 h later than the minimum value (250 m) measured by WPR. There is a large difference between the results of WPR/MWR and MPL, indicating that there are some shortages by using the aerosol scattering coefficient for defining the PBL height. For example, during night-time, the PBL height measured by MPL is much higher than that of MWR. The averaged heights are about 250–300 m measured by MWR and WPR. In contrast, the PBL heights are about 500–750 m measured by MPL. During day-time, however, the results are consistent for the all three instruments, indicating that MPL can be used to detect the PBL height during day-time (from 7 AM to 7 PM). This result suggests that: (1) the MWR and WPR instruments are suitable for detecting the PBL daily evolution, with the averaged PBL height being about 1000–1300 m during noon-afternoon-time, and 200–300 m during night-time measured in Tianjin in September; (2) the MPL instrument is only suitable for measuring the PBL height from 7 AM to 7 PM; and (3) although MWR and WPR show better ability for detecting the PBL diurnal variation, MPL also has its advantages for the PBL measurement, for example, MPL has higher temporal resolution than MWR and WPR (see Fig. 2), and renders clearer visualization than the direct measurements of MWR and WPR, which provide immediate information for the evolution of the PBL under different weather conditions.

3.2. Impacts of weather conditions on the evolution of the PBL

Table 1 shows several different weather conditions during the experiments, including clear sky, cloudy sky, haze, and rainy conditions. In this study, the haze condition is defined as the case when

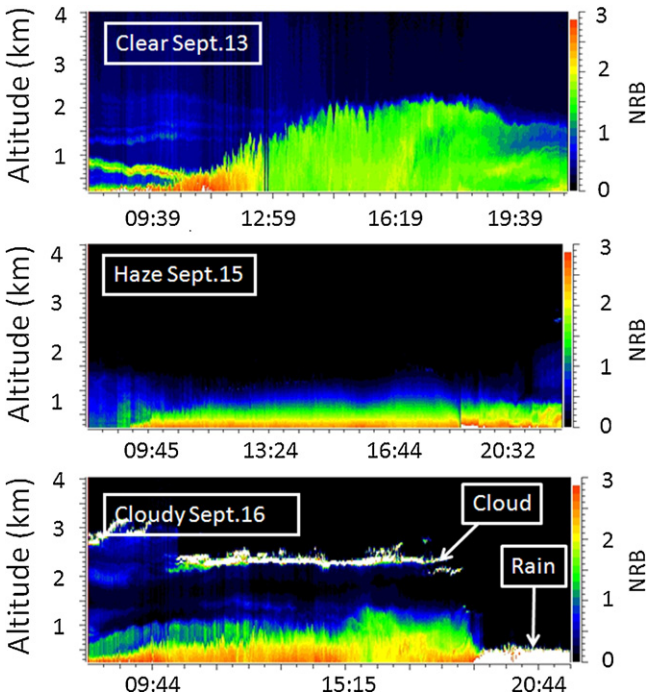

Fig. 2. Evolution of the PBL defined by the normalized relative backscatter (NRB, unit: count km^2/(μs μJ) of MPL on clear sky (13 September, upper panel), haze (15 September, middle panel), and cloudy sky (16 September, lower panel) conditions.

visibility is less than 5 km during non-fog days, in which the aerosol concentrations are normally very high. The aerosol mass concentration in this study is measured by SMPS, which only measures the particles with sizes ranging from 10 to 662 nm. Therefore the mass concentration shown in this study is lower than $PM_{2.5}$ concentration. Table 1 also shows the daily-averaged wind speed at altitude of 400 m observed by WPR during the experiments. The average wind speed was 2.7 m/s in haze condition, increased to 3.5 m/s in

Table 1
Weather situation, max PBL height and corresponding aerosol concentration during the experiments.

Date	Max PBL height[a] (m)	Aerosol[b] (μg/m^3)	Weather situation[c]	Wind speed (m/s)
9	950	43.7	Haze	3.64
10	1050	66.2	Haze	1.98
11	1500	13.3	Clear	2.00
12	1800	17.6	Clear	1.18
13	2000	31.1	Clear	0.91
14	1200	60.8	Haze	1.21
15	750	82.4	Haze or mist	1.99
16	950	33.9	Cloudy	3.93
17			Rain	6.64
18			Rain	7.43
19	1400	22.0	Clear	3.97
20	1200	56.8	Haze or mist	5.54
21			Rain	10.98
22	1700	7.0	Clear	5.57
23	2350	17.9	Clear	2.23
24	850	38.9	Haze	3.36
25	1600	13.0	Clear	4.32
26	1300	26.3	Clear	2.50
27		8.7	Clear (strong wind)	6.64
28	1800	12.7	Clear	5.98
29	1600	18.8	Cloudy	1.63
30	1600	52.3	Haze or mist	1.37

[a] Hourly averaged max PBL value.
[b] Hourly averaged aerosol concentration corresponding to the max PBL.
[c] Haze defined as visibility <5 km and mist as visibility <2 km.

Please cite this article in press as: Quan, J., et al. Evolution of planetary boundary layer under different weather conditions, and its impact on aerosol concentrations. *Particuology* (2012), http://dx.doi.org/10.1016/j.partic.2012.04.005

clear sky, and further increased to 8.3 m/s in rainy condition. During haze condition, the wind is weak, which is not favorable for the dispersion of air pollutants resulting in an enhancement of aerosol concentrations under the lower PBL condition (as shown in Table 1). During the rainy condition, the instruments cannot detect the PBL height, which is therefore excluded from the analysis. In order to analyze the impact of weather conditions, we show the PBL evolution under clear sky, haze, and cloudy sky conditions in Fig. 2 measured by MPL. As we described above, the MPL instrument is only suitable for measuring the PBL height during day-time, we will thus limit our analysis from 7 AM to 7 PM. Fig. 2 indicates that from 13 to 16 September, there is a strong transition from clear sky (13 September) to a haze condition (15 September) and then a cloudy condition (16 September). During this weather process the wind was weak (<2 m/s) and aerosol concentration increased gradually until 16 September.

Fig. 2 shows evidently that the evolution of the PBL was strongly affected by the weather conditions. During clear sky condition (13 September), the PBL pattern was typical. In the morning, the PBL height increased rapidly. At noon, the PBL height reached to 1 km, and continued to increase to about 1.2–1.8 km during afternoon. During the haze condition (15 September), the evolution of the PBL was strongly depressed by the haze condition (aerosol concentration of 82 μg/m^3). There was no clear diurnal pattern as indicated in the clear sky condition. As a result, the noon-time PBL height was only about 0.5–0.7 km, which was significantly lower than the clear sky condition. During the cloudy condition (16 September), the evolution of the PBL was strongly depressed by the cloud which was above the top of the PBL (around 2–2.5 km). The evolution of the PBL was weak and the noon-time PBL height was low (less than 1.0 km).

In order to analyze the effects of the weather conditions on the evolution of the PBL, Fig. 3 shows the measured heat flux (Q), friction velocity (u^*), turbulence kinetic energy (TKE) at 220 m on the meteorological tower from 13 to 17 September during the experiments. The result suggests that during daytime of the clear sky condition (13 September), both heat (Q) and momentum fluxes (TKE) were high, associated with higher atmospheric turbulence, leading to the rapid raise of the PBL height in noontime (about 2000 m). During daytime of the haze condition (15 September), the heat flux (Q) was significantly lower than that under clear sky condition. The momentum flux, however, was similar in magnitude compared to the clear sky condition. This result suggests that haze (or high aerosol loading) significantly reduced the solar radiation, leading to less heat turbulence in the PBL, which depressed the evolution of the PBL and resulted in the lower PBL height (about 750 m). During daytime of the cloudy condition (16 September), both the heat (Q) and momentum (TKE) fluxes were smaller than those under clear sky condition, but the heat (Q) flux was somewhat higher than that under haze condition. This result suggests that both the heat and momentum turbulences were depressed by clouds, which depressed the evolution of the PBL and resulted in the lower PBL height (about 950 m).

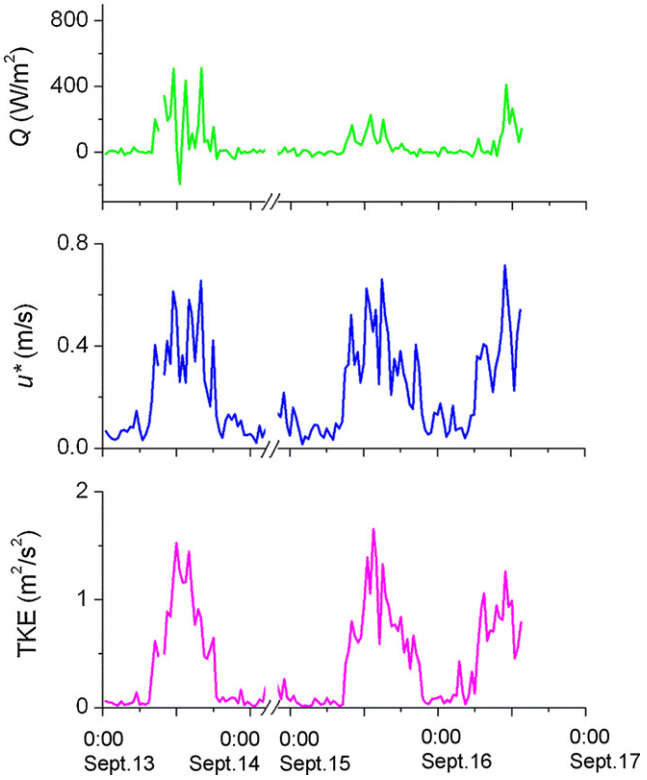

Fig. 3. Measured heat flux (Q), friction velocity (u^*), turbulence kinetic energy (TKE) at 220 m on the meteorological tower from 13 to 17 September during the experiments.

3.3. Impact of the PBL on air pollutants

Previous studies suggested that the evolution of the PBL has a significant effect on the surface air pollutants (Baumbach & Vogt, 2003; Han et al., 2009; Tie et al., 2007; Velasco et al., 2008). This study investigates the effect of the PBL under different weather conditions. Fig. 4 shows the existence of an anti-correlation between the PBL height and the aerosol concentration during clear and haze conditions. The average PBL heights were 1.08 and 1.70 km, whereas the average aerosol concentrations were 52 and 17 μg/m^3 under haze and clear sky conditions, respectively. The anti-correlation between the aerosol concentration and the PBL height reveals that a feedback loop may exist between aerosol and the PBL. Fig. 5 shows schematically this feedback action. When aerosol concentration was high, a haze condition could occur, which reduced incoming solar radiation on the surface. During daytime, less heating of the surface led to less turbulence due to the smaller heat flux (Q). As a result, the PBL height was lower than that under clear sky condition (as shown in Fig. 3). The lower PBL height can in turn depress aerosol in the PBL, leading to the increase in aerosol concentration. This process could form a positive feedback loop, leading to continuous increase in aerosol concentration, provided a haze condition lasted for several days. During the experiments, there were two continuous haze events: the first from 9 to 10 September, and the second from 14 to 15 September, both resulting in enhanced aerosol concentrations. For example, during the first event, the aerosol concentration increased from 43 to 66 μg/m^3, and during the second event, from 60 to 82 μg/m^3. However, the duration of the both haze events was only 2 days, and more experiments are therefore needed with longer haze events to provide more evidences for the existence of this positive feedback loop.

Fig. 6 shows that the evolution of the PBL was quite different under clear and haze conditions, leading to a strong impact on the diurnal variation of air pollutants. For example, under clear sky, the diurnal cycles of aerosol, SO_2, NO_x, and CO generally had two peak values: one in the morning (about 8–9 AM), and another in the evening or at night. The occurrence of the two peaks resulted from a combination of diurnal variations of emissions and PBL (Tie et al., 2007). Besides, Fig. 6 also indicates a minimum value of aerosols at the noontime due to the rapid increase of the PBL height under clear sky condition. In contrast, during haze condition, the diurnal variations of the air pollutants were different from those under

Please cite this article in press as: Quan, J., et al. Evolution of planetary boundary layer under different weather conditions, and its impact on aerosol concentrations. *Particuology* (2012), http://dx.doi.org/10.1016/j.partic.2012.04.005

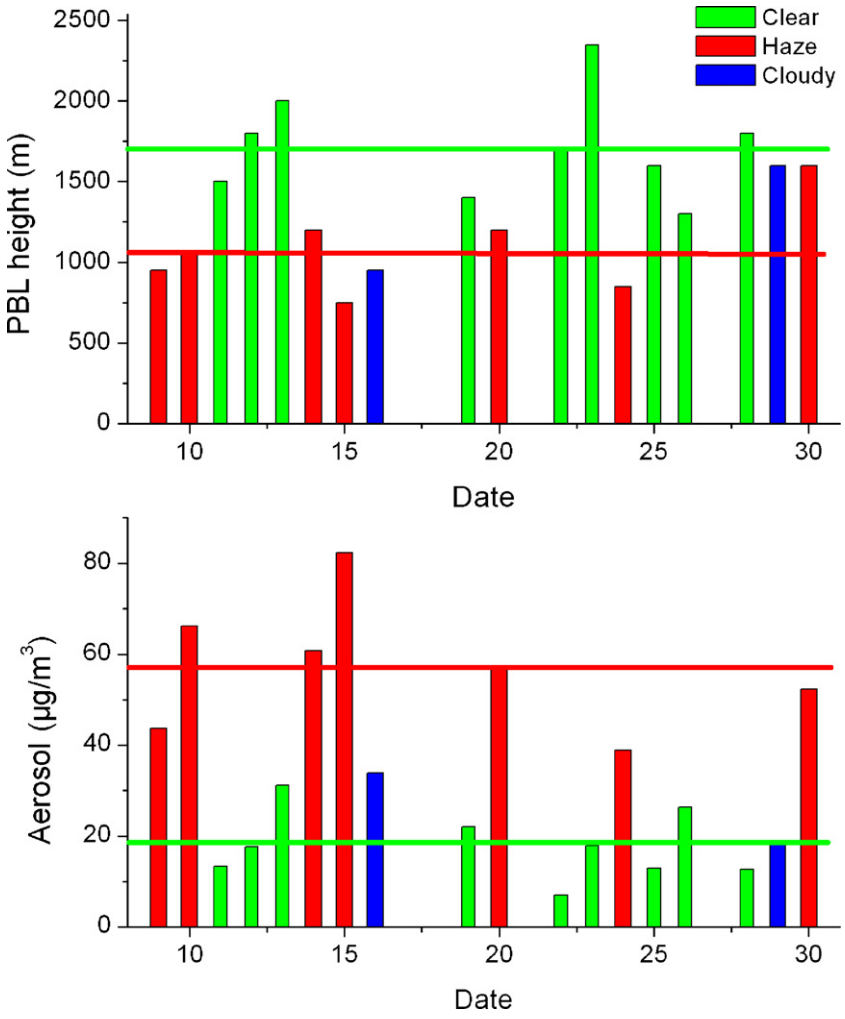

Fig. 4. The day-to-day variations of PBL height (upper panel) and aerosol concentration (lower panel) in September 2010 under different weather conditions.

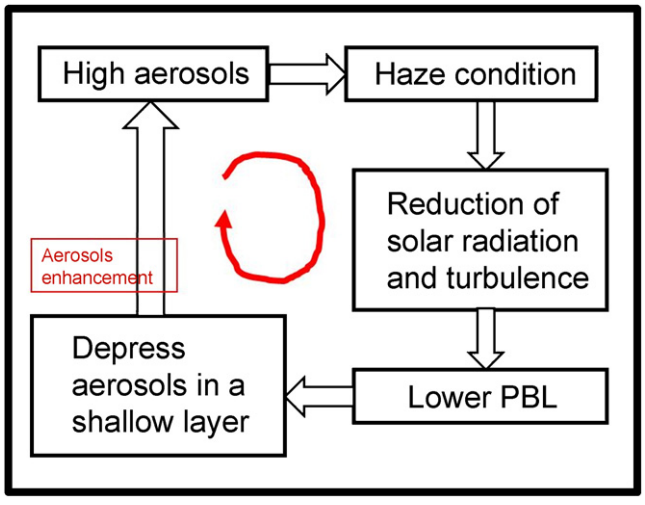

Fig. 5. Schematic for the existence of a positive feedback loop of aerosols and PBL evolution.

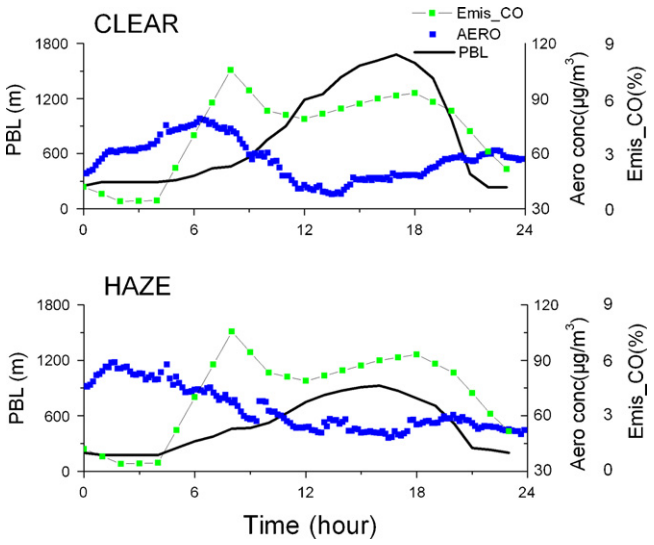

Fig. 6. The diurnal variations of PBL and air pollutants under clear and haze conditions.

Please cite this article in press as: Quan, J., et al. Evolution of planetary boundary layer under different weather conditions, and its impact on aerosol concentrations. *Particuology* (2012), http://dx.doi.org/10.1016/j.partic.2012.04.005

Table 2
Variations of PBL height, CO emission factor, and pollutants concentration at three periods.

Time (h)	PBL height (m)	Emis (CO)[a] (%)	CO (ppb)	Aerosols by SMPS ($\mu g/m^3$)
0:00–3:00 (P-1)	273.1	2.4	1417.3	51.2
6:00–9:00 (P-2)	367.9	19.8	1690	59
12:00–15:00 (P-3)	1371.1	16.3	1071	37.4
P-2/P-1	1.35	8.24	1.19	1.15
P-3/P-2	3.73	0.83	0.63	0.63

[a] Data from Tie et al. (2007).

the clear sky condition, for example, there were no the two peak values under haze condition and the noontime value of aerosol concentration ($60\ \mu g/m^3$) were significantly higher than the value ($40\ \mu g/m^3$) under clear sky condition. This result suggests that the change in the PBL diurnal variation under the haze condition had a harmful effect for human health at the noontime.

According the analysis by Tie et al. (2007), the dominant factors in controlling the diurnal variation of the PBL are the diurnal cycles of both PBL and emissions. In order to quantify the individual contribution from the two factors, Table 2 shows the emission rate and the PBL height during three periods, that is, period-1 (P-1, from 0:00–3:00), period-2 (P-2, from 6:00 to 9:00), and period-3 (P-3, from 12:00 to 15:00). Data for emission diurnal cycles are adopted from Tie et al. (2007). Table 2 shows that the CO and aerosol concentrations increased by 15–20% due to rapid increase of CO emission factor from P-1 to P-2. The PBL height also increased from P-1 to P-2, leading to reduction of the effect of the rapid increase of emission. From P-2 to P-3, the concentrations of CO and aerosol decreased by about 37%, mainly due to the sharp increase of the PBL height (increased by about of 370%), and to less extent, due to the decrease in the CO emission rate (decreased by about 17%). This analysis suggests that the noontime concentrations of air pollutants are strongly regulated by the PBL height, and better understanding of the evolution of the PBL height is very important for the regulation of air pollutants in large cities.

4. Summary

In this study, we compared the PBL determined by three remote sensing instruments and analyzed the relationship between PBL structure and aerosol loading based on field experiments conducted from 9 to 30 September 2010 at Tianjin, China. The results are summarized as the follows.

(1) There are differences between PBL heights determined by the three remote sensing instruments. MWR and WPR can be used to observe both daytime and nighttime PBL, except that the PBL height determined by WPR might be a little lower at day time, while for the MPL, it can only be used to observe daytime PBL.
(2) There might exist feedback between PBL height and aerosol loading. The enhancement of aerosols tends to depress the development of PBL by decreasing solar radiation, while the repressed structure of PBL will in turn weaken the diffusion of pollutants, leading to the heavy pollution. As a result, this possible positive feedback loop (more aerosols → lower PBL height → more aerosols) may induce an acceleration process for heavy ground pollution.

Acknowledgments

This research is partially supported by National Natural Science Foundation of China (NSFC) under Grant Nos. 41175007 and 40905060; the Project of Scientific and Technological New Star of Beijing under Grant No. 2010B029; the National Basic Research Program of China (2011CB403401); China Meteorological Administration (CMA) under Grant No. GYHY200806001-4.

References

Baumbach, G., & Vogt, U. (2003). Influence of inversion layers on the distribution of air pollutants in urban areas. *Water, Air and Soil Pollution*, *3*, 65–76.
Boers, R., & Eloranta, E. W. (1986). Lidar measurements of the atmospheric entrainment zone and the potential temperature jump across the top of the mixed layer. *Boundary-Layer Meteorology*, *34*, 357–375.
Bright, D. R., & Mullen, S. L. (2002). The sensitivity of the numerical simulation of the southwest monsoon boundary layer to the choice of PBL turbulence parameterization in MM5. *Weather and Forecasting*, *17*, 99–114.
Brooks, I. M. (2003). Finding boundary layer top: Application of a wavelet covariance transform to lidar backscatter profiles. *Journal of Atmospheric and Oceanic Technology*, *20*, 1092–1105.
Clifford, S. F., Kaimal, J. C., Lataitis, R. J., & Strauch, R. G. (1994). Ground-based remote profiling in atmospheric studies: An overview. *Proceedings of the IEEE*, *82*, 313–355.
Cohn, S. A., & Angevine, W. M. (2000). Boundary layer height and entrainment zone thickness measured by lidars and wind-profiling radars. *Journal of Applied Meteorology*, *39*, 1233–1247.
Dabberdt, W. F., Carroll, M. A., Baumgardner, D., Carmichael, G., Cohen, R., Dye, T., et al. (2004). Meteorological research needs for improved air quality forecasting: report of the 11th prospectus development team of the U.S Weather Research Program. *Bulletin of American Meteorological Society*, *85*, 563–586.
Geng, F., Zhang, Q., Tie, X., Huang, M., Ma, X., Deng, Z., et al. (2009). Aircraft measurements of O_3, NO_x, CO VOCs, and SO_2 in the Yangtze River Delta region. *Atmospheric Environment*, *43*, 584–593.
Guldner, J., & Spankuch, D. (1999). Results of year-round remotely sensed integrated water vapor by ground-based microwave radiometry. *Journal of Applied Meteorology*, *38*, 981–988.
Han, S. Q., Bian, H., Tie, X., Xie, Y., Sun, M., & Liu, A. (2009). Impact measurements of nocturnal planetary boundary layer on urban air pollutants: From a 250-m tower over Tianjin, China. *Journal of Hazardous Materials*, *162*, 264–269.
Hayden, K. L., Anlauf, K. G., Hoff, R. M., Strapp, J. W., Bottenheim, J. W., Wiebe, H. A., et al. (1997). The vertical chemical and meteorological structure of the boundary layer in the Lower Fraser Valley during Pacific 93. *Atmospheric Environment*, *31*(14), 2089–2105.
Hoff, R. M., Guise-Bagley, L., Staebler, R. M., Wiebe, H. A., Brook, J., Georgi, B., et al. (1996). Lidar, nephelometer and in situ aerosol experiments in Southern Ontario. *Journal of Geophysical Research*, *19*, 199–209.
Liu, H., Peters, G., & Foken, T. (2001). New equations for sonic temperature variance and buoyancy heat flux with an omnidirectional sonic anemometer. *Boundary-Layer Meteorology*, *100*, 459–468.
Schotanus, P., Nieuwstadt, F. T. M., & de Bruin, H. A. R. (1983). Temperature measurement with a sonic anemometer and its application to heat and moisture fluxes. *Boundary-Layer Meteorology*, *26*, 81–93.
Strawbridge, K. B., & Snyder, B. J. (2004). Planetary boundary layer height determination during Pacific 2001 using the advantage of a scanning lidar instrument. *Atmospheric Environment*, *38*, 5861–5871.
Tie, X., Madronich, S., Li, G. H., Ying, Z. M., Zhang, R., Garcia, A., et al. (2007). Characterizations of chemical oxidants in Mexico City: A regional chemical/dynamical model (WRF-Chem) study. *Atmospheric Environment*, *41*, 1989–2008.
Velasco, E., Márquez, C., Bueno, E., Bernabé, R. M., Sánchez, A., Fentanes, O., et al. (2008). Vertical distribution of ozone and VOCs in the low boundary layer of Mexico City. *Atmospheric Chemistry and Physics*, *8*(12), 3061–3079.
Westwater, E. R., Han, Y., Irisov, V. G., Leuskiy, V., Kadygrov, E. N., & Viazankin, S. A. (1999). Remote sensing of boundary layer temperature profiles by a scanning 5-mm microwave radiometer and RASS: Comparison experiments. *Journal of Atmospheric and Oceanic Technology*, *16*, 805–818.
Wilczak, J. M., Gossard, E. E., Neff, W. D., & Eberhard, W. L. (1996). Ground-based remote sensing of the atmospheric boundary layer: 25 years of progress. In J. R. Garratt, & P. A. Taylor (Eds.), *Boundary-Layer Meteorology*. Kluwer Academic Publishers 25th Anniversary.
Wyngaard, J. C. (1990). Scale fluxes in the planetary boundary layer theory, modeling and measurement. *Boundary-Layer Meteorology*, *50*, 49–75.

Please cite this article in press as: Quan, J., et al. Evolution of planetary boundary layer under different weather conditions, and its impact on aerosol concentrations. *Particuology* (2012), http://dx.doi.org/10.1016/j.partic.2012.04.005

Ying, Z. M., Tie, X., & Li, G. H. (2009). Sensitivity of ozone concentrations to diurnal variations of surface emissions in Mexico City: A WRF/Chem modeling study. *Atmospheric Environment*, *43*, 851–859.
Zhang, Q., Ma, X., Tie, X., Huang, M., & Zhao, C. (2009). Vertical distributions of aerosols under different weather conditions: Analysis of in situ aircraft measurements in Beijing China. *Atmospheric Environment*, *43*, 5526–5535.
Zhang, Q., Quan, J., Tie, X., Huang, M., & Ma, X. (2011). Impact aerosol particles on cloud formation: Aircraft measurements in Beijing China. *Atmospheric Environment*, *45*, 665–672.

Please cite this article in press as: Quan, J., et al. Evolution of planetary boundary layer under different weather conditions, and its impact on aerosol concentrations. *Particuology* (2012), http://dx.doi.org/10.1016/j.partic.2012.04.005